

## Supporting Information

### Mechanical Regulation of the Cytotoxic Activity of Natural Killer Cells

Lital Mordechay<sup>1,2</sup>, Guillaume Le Saux<sup>1,2</sup>, Avishay Edri<sup>3</sup>, Uzi Hadad<sup>2</sup>, Angel Porgador<sup>3</sup>, Mark Schvartzman<sup>1,2\*</sup>

<sup>1</sup>Department of Materials Engineering, <sup>2</sup>Ilse Katz Institute for Nanoscale Science & Technology, <sup>3</sup>The Shraga Segal Department of Microbiology, Immunology and Genetics, Faculty of Health Sciences, Ben-Gurion University of the Negev, Beer Sheva, Israel.

\*Corresponding author

#### Measurements of PDMS Stiffness

Elastic moduli of PDMS were determined from the slopes of force-distance curves (**Figure S1.a**) using AFM (Asylum Research, MFP-3D-Bio, Hertz model).<sup>1-3</sup> At least 10 measurements were taken for each sample. All the measurements were taken with the same AFM probe type (AC240TS, Olympus,  $k=1.4\text{N/m}$ ). The Poisson ratio of 0.45 for PDMS was used for the modulus calculation.<sup>4-6</sup> Notably, the curves for the soft and medium samples (curves a and b) show inflection points in an elbow shape, indicating that there might be some depth effect on the rigidity measurement. Thus, for the stiffness measurements, we analyzed only the shallow indentation for these samples. To eliminate a possible effect of plasma treatment and surface functionalization on the surface stiffness, we measured the stiffness of a sample in the range of  $\sim 30\text{ kPa}$  before the plasma treatment, after the plasma treatment, and after APTES immobilization

(**Figure S1.b**). All the measurements were taken using AFM (Nanosurf, ANA, Hertz model) with the same AFM probe type (PPP-XYCONTR, Nanosensors,  $k=0.2\text{N/m}$ ).

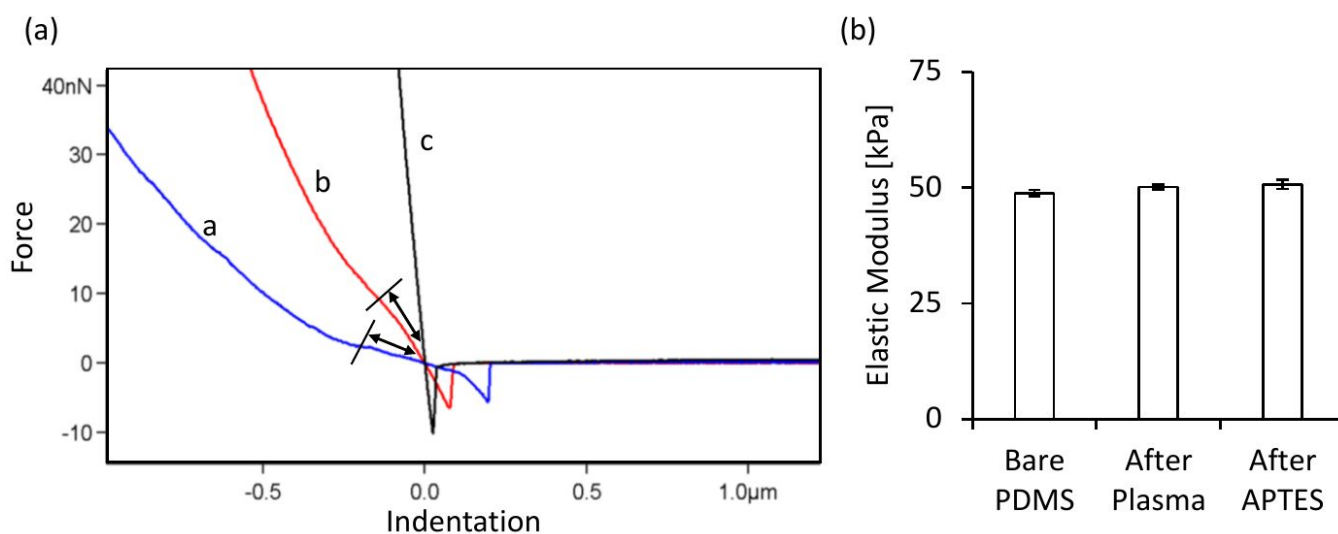


*Figure S1: (a) AFM force-distance curves for three PDMS samples prepared using different hardener-resin ratios and curing temperatures: (a) 1:50,  $130^{\circ}\text{C}$  (b) 1:35,  $130^{\circ}\text{C}$  (c) 1:10,  $200^{\circ}\text{C}$ . Arrows indicate shallow indentations. (b) Elastic moduli of the softer stiffness. The stiffnesses were measured on bare PDMS and after each step of the biofunctionalization.*

#### Assessment of MICA Density by Fluorescence

The surface density of MICA for each sample was quantified by fluorescence. First, a  $0.5\mu\text{L}$  drop of TAMRA-MICA at a concentration of  $2\mu\text{g/mL}$  was cast on a clean glass slide and left to dry. The intensity of the remaining fluorescent stain was quantified and used as a standard (**Figure S2.a**). The fluorescence intensity of TAMRA-MICA was measured on each PDMS surface, and the corresponding surface density of MICA was calculated based on the reference (**Figure 1.a**).

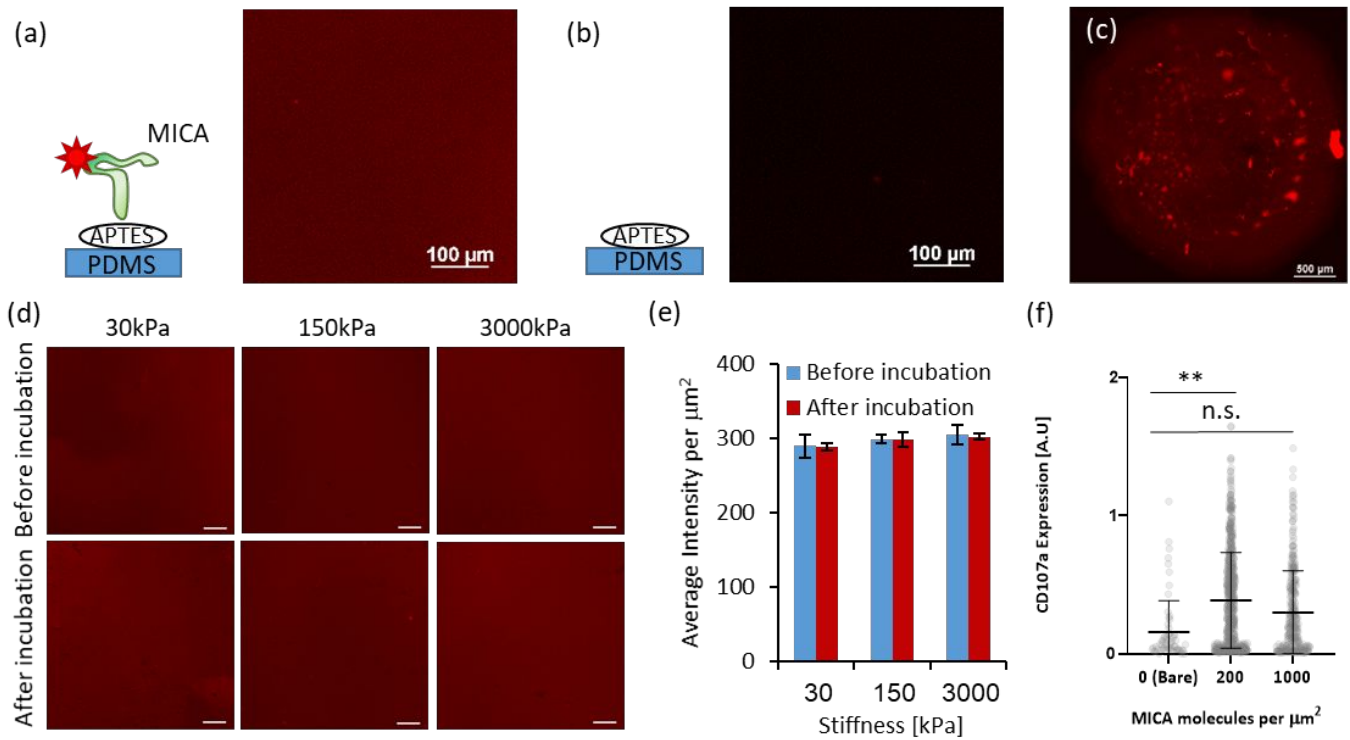


Figure S2: (a - b) Fluorescence images of PDMS substrates functionalized with (a) APTES only and (b) APTES followed by TAMRA-labeled MICA. The pictures are shown here have the same contrast range. (c) Fluorescence image of TAMRA-MICA on glass, used as a reference for quantification of MICA molecules which shown in **Figure 1.a**. (d) Representative images of all the surfaces which shown in (c). Scale bar: 200 $\mu\text{m}$ . (e) The stability of MICA molecules on the surface. Average fluorescence intensity of TAMRA-MICA before and after incubation, for all the stiffnesses (30 kPa, 150 kPa and 3MPa). (f) Activation level of NK cells on 150kPa PDMS with different surfaces concentration of MICA.

### Statistics

Fluorescence data was quantified using the ImageJ (Fiji) imaging software (<https://fiji.sc>).

Statistical analysis was performed by using GraphPad Prism, analysis of variance and Tukey's multiple-comparison post hoc tests were performed to assess the

significant changes in behavior - the results were considered to be significantly different for  $p < 0.05$ .

### Activation of NK Cells

The degree of NK cell activation was quantified from the intensity of the APC-labelled anti-CD107a signal in each cell. For this, the exposure time was optimized once on the first sample and then locked for each experiment, and at least 10 fields at 20× magnification on each surface were analyzed. The data were averaged for each experiment, at least three sets of samples per experiment were performed, and at least three different experiments were performed. A minimum of 200 cells was analyzed per type of sample.

### Control Experiment with Cytoskeletal Inhibitors

To examine the function of actin and myosin, pNK was treated for 30 minutes with actin inhibitors, 7mM latrunculin A (Caymanchem),<sup>7</sup> 10mM cytochalasin D (Caymanchem),<sup>8</sup> and myosin inhibitor, 75mM blebbistatin in 0.3% DMSO (Sigma-Aldrich).<sup>9</sup> Then, the cells were incubated on the samples in the same process as in the activation experiments.

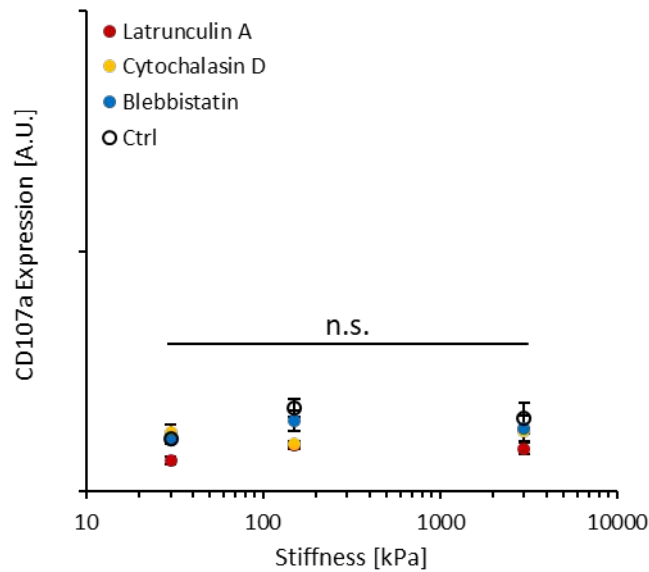


*Figure S3: Degree of CD107a cell-surface expression of NK cells on bare PDMS, with drug treatments of latrunculin A, cytochalasin D, blebbistatin and control (ctrl) without pre-treatment, as in the activation experiments. The degree of CD107a was quantified by summarizing the fluorescence intensity of the APC-labeled anti-CD107a per cell. The results show the compilation of more than 20 cells per sample. Using GraphPad Prism, analysis of variance and Tukey's post hoc tests were performed to assess the significant changes in behavior of  $p < 0.05$ .*

#### Quantification of NK Cell Response to Inert Surface Chemistry

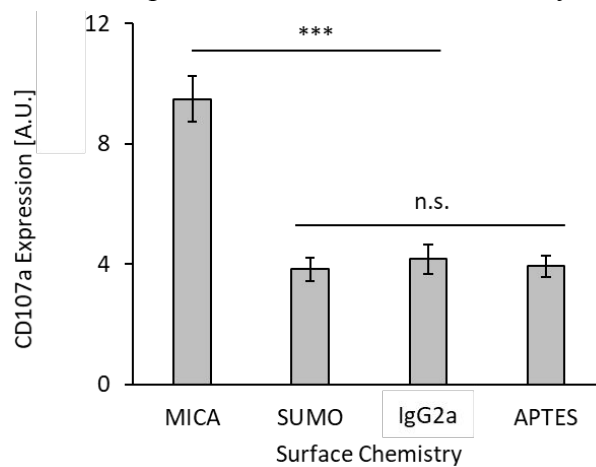


*Figure S4: NK cell immune response to various types of surface chemistry on PDMS with 150kPa stiffness. The degree of CD107a was quantified by summarizing*

*the fluorescence intensity of the APC-labeled anti-CD107a per cell. The results show the compilation of at least 300 cells from three different experiments and for three sets of samples per experiment. Using GraphPad Prism, analysis of variance and Tukey's post hoc tests were performed to assess the significant changes in behavior – four stars (\*\*\*) represent  $p < 0.001$ .*

### Spreading of NK Cells

The values for the spreading and activation gates for the 2D spreading-activation density plots (**Figure 2.c**) were determined as the average + standard error of the cell area and CD107a signals on bare PDMS and were equal to  $200\mu\text{m}^2$  and 25000 a.u., respectively.

### Quantification of NKG2D Expression

NKG2D expression was varied within the primary natural killer cell population in culture. Primary NK cells were stained with Allophycocyanin (APC)-conjugated anti-human NKG2D. Dead cells were excluded using 7AAD viability staining.

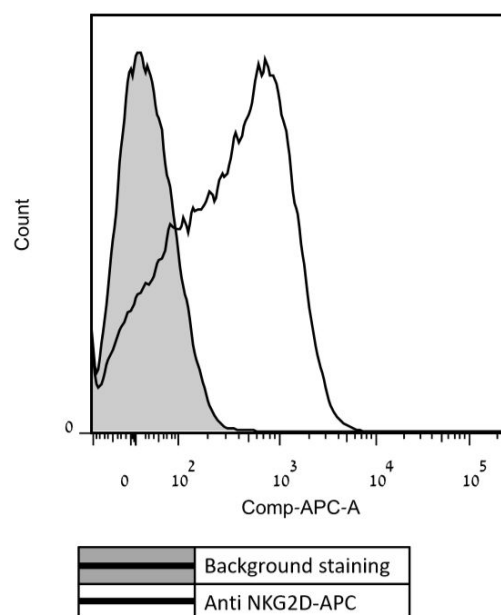


*Figure S5: Depicting pNK staining with anti-NKG2D-APC.*

#### Quantification of DAP10 Clustering

For DAP10, quantification of fluorescence intensity, exposure time, detector gain, and laser power were optimized once on the first sample and then locked.

The DAP10 nanoclusters were analyzed by ImageJ analysis software. A Gaussian filter ( $\sigma=4$ ) was applied to the Airyscan image, and then the filtered image was subtracted from the original one, resulting in an image of the clusters. The area of DAP10 clusters was calculated by analyzing the binary color map, with a feature size threshold of  $0.03\mu\text{m}^2$ . The threshold was determined from the resolution limit of the microscope ( $\sim 140$  nanometers, depending on the wavelength). The analysis was extracted from the unfiltered image with the calculated cluster areas. The results show the compilation of more than ten cells per sample. A minimum of 50 clusters was analyzed per cell.

#### Proposed Model for NKG2D Mechanosensing

The proposed catch-bond mechanism of NKG2D-MICA can explain the observed bell-shape response, but still needs to be verified.

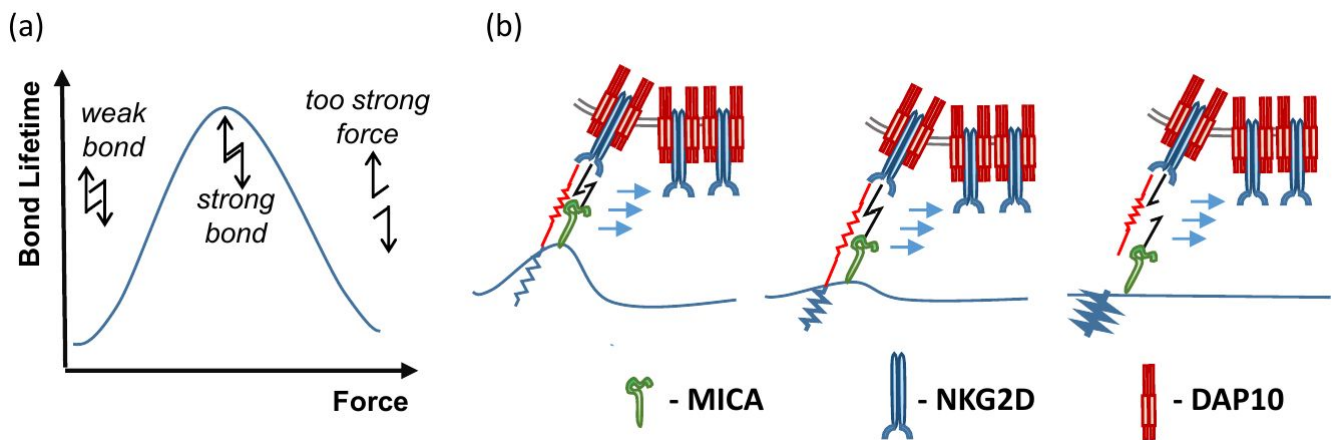


*Figure S6: (a) Scheme of catch-bond lifetime vs. applied force. (b) Proposed model for the effect of surface stiffness on the receptor clustering.*

## References

- (1) Leadley, S.; O'Hare, L.-A.; McMillan, C. *Surface Analysis of Silicones*; 2012.
- (2) Cappella, B. *Mechanical Properties of Polymers Measured through AFM Force-Distance Curves*; 2016.
- (3) Saitakis, M.; Dogniaux, S.; Goudot, C.; Bufi, N.; Asnacios, S.; Maurin, M.; Randriamampita, C.; Asnacios, A.; Hivroz, C. Different TCR-Induced T Lymphocyte Responses Are Potentiated by Stiffness with Variable Sensitivity. *Elife* **2017**, 6, 1–29.
- (4) Seghir, R.; Arscott, S. Extended PDMS Stiffness Range for Flexible Systems. *Sensors Actuators, A Phys.* **2015**, 230.
- (5) Cesa, C. M.; Kirchgeßner, N.; Mayer, D.; Schwarz, U. S.; Hoffmann, B.; Merkel, R. Micropatterned Silicone Elastomer Substrates for High Resolution Analysis of Cellular Force Patterns. *Rev. Sci. Instrum.* **2007**, 78 (3).
- (6) Johari, S.; Fazmir, H.; Anuar, A. F. M.; Zainol, M. Z.; Nock, V.; Wang, W. PDMS Young's Modulus Calibration for Micropillar Force Sensor Application. *RSM 2015 - 2015 IEEE Reg. Symp. Micro Nano Electron. Proc.* **2015**, No. October 2017.
- (7) Mace, E. M.; Wu, W. W.; Ho, T.; Mann, S. S.; Hsu, H.-T.; Orange, J. S. NK Cell Lytic Granules Are Highly Motile at the Immunological Synapse and Require F-Actin for Post-Degranulation Persistence. *J. Immunol.* **2012**, 189 (10), 4870–4880.
- (8) Rak, G. D.; Mace, E. M.; Banerjee, P. P.; Svitkina, T.; Orange, J. S. Natural Killer Cell Lytic Granule Secretion Occurs through a Pervasive Actin Network



at the Immune Synapse. *PLoS Biol.* **2011**, 9 (9).

- (9) Andzelm, M. M.; Chen, X.; Krzewski, K.; Orange, J. S.; Strominger, J. L.  
Myosin IIA Is Required for Cytolytic Granule Exocytosis in Human NK Cells.  
*J. Exp. Med.* **2007**, 204 (10), 2285–2291.